Title

Preclinical Evaluation of a Single Intravenous Infusion of hUC-MSC (BX-U001) in Rheumatoid Arthritis

Permalink

https://escholarship.org/uc/item/3v2539wc

Authors

Liu, Linan
Farhoodi, Henry P
Han, Menglu
et al.

Publication Date

2020

DOI

10.1177/0963689720965896

Peer reviewed

Preclinical Evaluation of a Single Intravenous Infusion of hUC-MSC (BX-U001) in Rheumatoid Arthritis

Linan Liu[1],*, Henry P. Farhoodi[2,3,4],* ⓘ, Menglu Han[2,3,4],
Guangyang Liu[5], Jingxia Yu[5], Lily Nguyen[2,3,4],
Brenda Nguyen[2,3,4], Agnes Nguyen[2,3,4], Wenbin Liao[1],
and Weian Zhao[2,3,4,6,7,8]

Abstract

Rheumatoid arthritis (RA) is an inflammatory disease of the joints, which causes severe pain and excessive systemic circulation of harmful inflammatory cytokines. Current treatments are limited, with some patients not responding well, and some experiencing severe and detrimental side effects. Mesenchymal stem cells (MSC) are cell-based therapeutics being evaluated as potent immunomodulators in RA and may provide relief to patients not responding well to drug-based treatments. We evaluated the safety and efficacy of BX-U001 human umbilical cord tissue–derived mesenchymal stem cells (hUC-MSC) to treat RA, in support of a successful investigational new drug application. A collagen-induced arthritis (CIA) mouse model of RA was established in DBA/1 J mice. Mice from the treatment assessment group were given a tail vein infusion of hUC-MSC 24 days after primary RA induction, while control assessment (CA) group mice were given cell-free carrier solution. All animals were evaluated daily for RA symptoms via clinical scoring, blood was taken periodically for cytokine analysis, and mice were dissected at end point for histological analysis. A linear mixed model was used to compare the rate of change among groups. The clinical scores of TA group were significantly reduced compared with CA group ($P < 0.01$), indicating therapeutic effects. The histological scores of the joints in TA group were significantly lower than those in the CA group ($P < 0.05$), but had no significant difference compared with Healthy groups ($P > 0.05$). The concentration of (interleukin) IL-6 in TA group was significantly reduced by 80.0% ($P < 0.0001$) 2 days after treatment and by 93.4% at the experimental endpoint compared with levels prior to hUC-MSC injection. A single intravenous infusion of hUC-MSC (2×10^6 cells/mouse), to CIA-induced DBA/1 J mice, resulted in significant alleviation of RA symptoms and may provide significant therapeutic benefits in humans.

[1] Baylx, Inc., Irvine, CA, USA
[2] Sue and Bill Gross Stem Cell Research Center, University of California, Irvine, CA, USA
[3] Department of Pharmaceutical Sciences, University of California, Irvine, CA, USA
[4] Chao Family Comprehensive Cancer Center, University of California, Irvine, CA, USA
[5] Department of Surgery, University of California, Irvine, Orange, CA, USA
[6] Edwards Life Sciences Center for Advanced Cardiovascular Technology, University of California, Irvine, CA, USA
[7] Department of Biomedical Engineering, University of California, Irvine, CA, USA
[8] Department of Biological Chemistry, University of California, Irvine, CA, USA
*Both the authors contributed equally to this article

Corresponding Author:
Weian Zhao, Sue & Bill Gross Hall CIRM Institute, 845 Health Sciences Road, Suite 3027, Irvine, CA 92697, USA; Wenbin Liao, Baylx, Inc., 1 Technology Dr c511, Irvine, CA 92697, USA.
Emails: weianz@uci.edu; wliao@baylxinc.com

Introduction

Arthritis affects over 54 million Americans and can lead to rheumatoid arthritis (RA)[1,2]. RA is an inflammatory disease that affects between 1.5 and 3 million Americans and is characterized by inflammation of the synovial and cartilage tissue, causing damage to the articular cartilage and bone[3–8]. RA can lead to reduced quality of life and serious damage to organ systems, caused by the high level of inflammatory cytokines circulating in the blood[9,10]. The causes of RA are still being elucidated, but there is a clear inflammatory cascade that involves the production of tumor necrosis factor alpha (TNF-α) and interleukin 6 (IL-6), following the production of autoantibodies including "Rheumatoid Factor" and anti-citrullinated protein autoantibodies[5,6,11]. The proinflammatory cytokines and autoantibodies activate macrophages to infiltrate and damage the tissues of the joint, while simultaneously producing more inflammation[12–15]. There are also autoantibody-negative cases of RA, in which disease is characterized by inflammation and fibrosis, developed from the infiltration of fibroblast-like synoviocytes and increased thickening of synovial lining[16,17]. While autoantibody-positive RA is associated with worse prognosis, both types of disease result from macrophage-dependent inflammation[12–18].

One of the problems with treating autoimmune diseases, such as RA, is that the immune system is complex, and pharmaceutical drugs and biologics tend to target only one or a small subset of the system[19]. The current standard treatment regime varies by country, but is generally reliant on methotrexate and biologics (for instance, antibodies against TNF-α), but nonsteroidal anti-inflammatory drugs and corticosteroids are still common treatments[20]. These treatments are not at all targeted toward the specific causes of RA, cause immunosuppression, and have significant side effects[21,22]. There is great need for more effective therapeutics, and treatments that do not produce systemic immunosuppression[23].

Stem cell therapies have the potential to treat and manage autoimmune disorders in ways that conventional drugs cannot, because stem cells can harness the complex mechanisms that the body naturally uses to modulate and restore the imbalanced immunity with minimal toxicity[21]. In particular, mesenchymal stem cells (MSC) have been shown to have immunomodulatory effects on many types of immune cells and have limited side effects in past preclinical and clinical studies[22]. MSC are multipotent cells that can be readily isolated from many different adult tissues including fat, bone marrow, blood, and umbilical cord[21]. These cells can then be expanded *in vitro* to serve as "off-the-shelf" therapeutics. Human umbilical cord tissue–derived MSC (hUC-MSC) have been shown to have strong immunomodulatory effects and may have higher therapeutic potential for RA than bone marrow–derived MSC[22]. Due to MSC's immune-evasive and immunomodulatory properties, they do not have the major graft-vs-host issues that other cell types do, making them amenable to allogenic transplantation. MSC have been shown to affect CD4+/CD8+ T cells, T regulatory cells (T-reg), B cell, monocytes, natural killer cells, and macrophages. The immunomodulatory mechanism of action is by direct contact inducing apoptosis of effector lymphocytes, and secretion of soluble mediators such as indoleamine 2,3-dioxygenase, prostaglandin E2, IL-6, and HLA-G5, which are known to dampen immune response[24]. This multi-pronged immunomodulatory power makes these cells capable of treating diseases caused by many different cell types. Previous preclinical animal studies have consistently shown reduction of RA symptoms upon treatment with MSC, regardless of the animal model used[22]. This preclinical study evaluates the potential of a new MSC product derived from human umbilical cord tissue (BX-U001) to treat a collagen-induced arthritis (CIA) mouse model of RA, and led to the successful filing of an investigational new drug (IND) application with the US Food and Drug Administration to initiate a clinical trial.

Materials and Methods

Isolation and Culture of hUC-MSC

The hUC-MSC used in this study were isolated and cultured from umbilical cord tissue by a standard tissue explant method[25]. Cells were cultured in hUC-MSC growth medium (Baylx, USA) at 37°C in 5% CO_2. Cells were used in experiments at passage 6 from tissue harvest.

hUC-MSC Differentiation Assays

For osteogenic and adipogenic differentiations, hUC-MSC were seeded onto 24-well tissue culture plates with 6×10^4 cells/well and incubated at 37°C in a humidified atmosphere containing 5% CO_2. The differentiation induction medium from the Mesenchymal Osteogenesis Differentiation Kit and Mesenchymal Adipogenesis Differentiation Kit (EMD Millipore, Germany) were added after the confluence reached 90%. The medium was changed every 2 to 3 days based on the manufacturer's protocol and adipogenic differentiation was confirmed by the deposition of lipid droplets in the cytoplasm using Oil Red O staining (EMD Millipore, Germany). The osteogenic differentiation was confirmed by positive staining of the extracellular calcium matrix using Alizarin Red S staining (EMD Millipore, Germany). Images of the stained samples were collected using a Nikon Ti-E microscope (Nikon, Japan).

Flow Cytometry

The phenotype of hUC-MSC was analyzed by flow cytometry after trypsinization. MSC were stained with fluorescein isothiocyanate-conjugated antibodies against CD34 and HLA-DR, or phycoerythrin-conjugated antibodies against CD45, CD90, CD105, and CD73. Mouse isotypic antibodies served as the control. Cells were stained in single label according to the manufacturer's instructions and then analyzed by flow cytometry on a BD Accuri C6 flow cytometer

Table 1. Animal Grouping.

Group	Agent name	Dosage (cells)	Volume of infusion	Animal number
CA	Cell-free carrier solution	-	200 μl/mouse	20
TA	hUC-MSC injection	2×10^6/mouse	200 μl/mouse	21
Healthy	-	-	-	7

CA: control assessment; hUC-MSC: human umbilical cord tissue–derived mesenchymal stem cells; TA: treatment assessment.
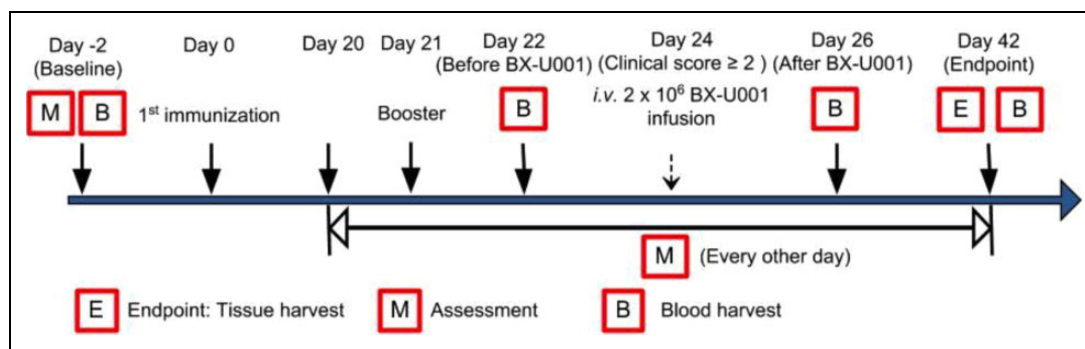
Figure 1. Timeline of using human umbilical cord tissue–derived mesenchymal stem cells to treat collagen-induced rheumatoid arthritis.

(BD Biosciences, USA). Flow cytometry data were processed using FlowJo (FlowJo, USA).

hUC-MSC Potency Assay

hUC-MSC (1×10^4 cells/well) were co-cultured with anti-CD3/anti-CD28/IL-2 treated human PBMC (1×10^5 cells/well) in 96-well tissue culture plates. Activated PBMC cultured alone were used as positive control (control non-MSC, secretion inhibition efficiency = 0%). The TNF-α expression was then measured with a LEGEND MAX Human TNF-α ELISA Kit (Biolegend, USA) after 3 days' co-culture.

Animal Studies

A total of 60 male DBA/1 J mice (Jackson Laboratories, USA) were randomly labeled and used for 2 identical experiments. Of those 60, 53 animals were selected randomly for primary induction (26 mice in the first study [Batch 1] and 27 mice in the second [Batch 2]). The remaining 7 mice were assigned to Healthy groups. On the day of hUC-MSC infusion, 41 mice met the disease-onset criteria (i.e., at least 1 leg reached the clinical score ≥2 on the day of infusion) and mice were regrouped randomly to ensure no significant differences of clinical scores existed between TA and CA groups. There were 21 mice in TA group (11 in Batch 1 and 10 in Batch 2), 20 in CA group (10 in Batch 1 and 10 in Batch 2), and 7 in Healthy group (4 in Batch 1 and 3 in Batch 2) (Table 1). Body weight (17 to 23 g for Batch 1; 16 to 24 g for Batch 2) of animals was measured every 3 days from the start of baseline blood collection (2 to 3 days before primary induction), to 18 days after the primary

induction (Day 18), and was measured every other day thereafter (Fig. 1). The mice were monitored daily and assessed every other day, in a double-blind fashion, for signs of arthritis onset (based on clinical scores) by two independent investigators. Clinical arthritis was scored on a scale of 0 to 4, where 0 =no swelling, 1 =erythema and mild swelling limited to tarsals or ankle joint, 2 =erythema and mild swelling extending from ankle to tarsal joints, 3 =erythema and moderate swelling extending from ankle to metatarsal joints, and 4 =erythema and severe swelling surrounding the ankle, foot, and digits, or ankylosis of the limb. Each limb was graded and the grades from four limbs were summed to yield the arthritis score for each animal. The maximal score was 16. Paw thickness (exploratory outcome) was also assessed with a 0 to 10 mm Thickness Gage (Mitutoyo, Japan). All animals were sacrificed 42 days after primary induction (Day 42, end point) with CO_2 (or isoflurane) overdose and cervical dislocation. Legs were harvested for further processing, followed by mouse dissection. Notes were taken and a histopathological exam was conducted if any abnormality in the volume, color, texture, and so on of organs (brain, heart, liver, spleen, lung, kidney, and injection-site tissue) was observed. All animal experiments and procedures were performed under permission from the UCI Institution of Animal Care and Use Committee (IACUC protocol number AUP-19-082) and conducted per the Animal Welfare Assurance (#A3416.01).

Arthritis Induction

For CIA, DBA/1 J mice were immunized with 100 μg of bovine type II collagen (Chondrex, USA), which was

emulsified with Freund's complete adjuvant containing 200 μg of *Mycobacterium tuberculosis* H37Ra (Sigma-Aldrich, Germany), via an intradermal injection at the base of the tail; and a booster emulsion of CII in Freund's incomplete adjuvant was administered at 21 days (Day 21) after the primary immunization (Fig. 1)[26]. Disease onset was defined as at least one leg reaching the clinical score ≥2.

MSC Administration

At 24 days (Day 24) after primary induction of CIA (after disease onset), a single infusion of 200 μl carrier solution (Baylx, USA) or 2 million hUC-MSC suspended in 200 μl carrier solution (1×10^7 cells/ml) was intravenously infused via tail vein to each mouse from CA and TA groups. Intravenous infusion via tail vein was used to mimic the clinical administrative route and was done with 1 ml sterile syringes with 30 G × ½ disposable needles and an infusion speed of 8 to 20 μl/s. After drug administration, animals were closely monitored for 2 h. If any abnormality was observed (e.g., any profound paralysis that inhibits animals' ability to eat or drink, any signs of pain including piloerected/unkempt fur, squinted eyes, ataxia, hunched posture, labored breathing, which is not relieved with analgesia), symptoms and their starting time, severity, duration, and so on were recorded in detail. Thereafter, monitoring was also conducted twice a day with notes taken accordingly.

Serum Cytokine Quantification

Murine blood was collected into ethylenediamine tetraacetic acid (EDTA)-coated collection tubes (Sai-infusion, USA) at baseline (2 to 3 days before primary induction), before treatment (Day 22), after treatment (Day 26), and at end point (Day 42) (Fig. 1). Then the sera were harvested from blood samples after centrifugation. The pro-inflammatory cytokine levels (including IL-1β, TNF-α, interferon gamma [IFN-γ], and IL-6) were determined by a MILLIPLEX MAP Mouse TH17 Magnetic Bead Panel Luminex assay (EMD Millipore, Germany) following the manufacturer's protocol.

Tissue Processing and Histology

Excessive fur and muscle were removed with scissors and tweezers from each mouse's limbs before being fixed in 10% formalin for 2 days. The limbs were decalcified for 3 to 4 weeks in decalcification solution (14% EDTA, 0.2% of 4% paraformaldehyde in 1× phosphate-buffered saline, pH = 7.4); the decalcification solution was changed every 2 to 3 days. All limbs were processed in a TP1020-1-1 tissue processor (Leica, Germany) using an 18-h processing protocol. The 10-μm paraffin sections were stained using hematoxylin and eosin (H&E; EMD Millipore, Germany) to assess the difference in tissue morphology among TA, CA, and Healthy groups. Stained tissue was imaged on a Nikon Ti Eclipse (Nikon, Japan) using a 10× objective. Representative images

of H&E-stained limbs from all three groups were independently scored by two blinded investigators on a scale from 0 to 4, where 0 = no cell infiltration, cartilage damage, or bone erosion; 1 = mild cell infiltration and synovial membrane hypertrophy, and little to no cartilage damage; 2 = obvious cell infiltration, mild cartilage damage, and little to no bone erosion; 3 = severe cell filtration, cartilage erosion, and bone erosion; and 4 = complete loss of joint integrity and ankylosis. Representative images are shown in Fig. 2 and average histology scores are shown in Table 2.

Data Analysis and Statistics

Data were analyzed by Student's two-tailed t test when comparing two groups. Data were expressed as the mean ± standard error of the mean, mean ± standard deviation of the mean, and 95% confidence interval (95% CI), and differences were considered significant at $P < 0.05$. CIA mice that did not meet the disease-onset criteria for treatment (i.e., at least one leg has a clinical score ≥2) on the infusion day were removed from the study. Samples with failed readings or out of the upper limit of standard curve in Luminex assay were removed from the analysis. Luminex readings out of the lower limit of the standard curve were defined as "0". See Supplementary Materials for detailed information for analysis on clinical scores and paw thickness.

Results

Generation and In Vitro Characterization of hUC-MSC

The hUC-MSC used in this study were generated from umbilical cord tissue and were characterized to have standard MSC phenotype according to the International Society for Cellular Therapy criteria (Fig. 3). We established a laboratory cell bank of hUC-MSC at passage 5. This cell bank was used for *in vitro* characterization and for the animal experiments in our IND-enabling studies. The hUC-MSC cell line displayed appropriate marker expression (Fig. 3A). The hUC-MSC showed high expression of the key MSC markers CD73, CD90, and CD105, while maintaining low expression of non-MSC markers including CD45, CD34, and HLA-DR. Multipotency was displayed via adipogenesis and osteogenesis (Fig. 3B). When co-cultured with activated PBMC, the hUC-MSC reduced TNF-α inflammatory cytokines by over 10-fold (Fig. 3C), indicating an anti-inflammatory functional potency.

hUC-MSC Improved Arthritis Assessment Outcomes

CIA was established in DBA/1 J mice to mimic human RA. CIA animals were grouped randomly into either a treatment assessment (TA) group, which received a tail vein infusion of 2 million hUC-MSC or a control assessment (CA) group, which received only cell-free carrier solution.

To evaluate disease severity and treatment efficacy, clinical assessments were taken by two independent
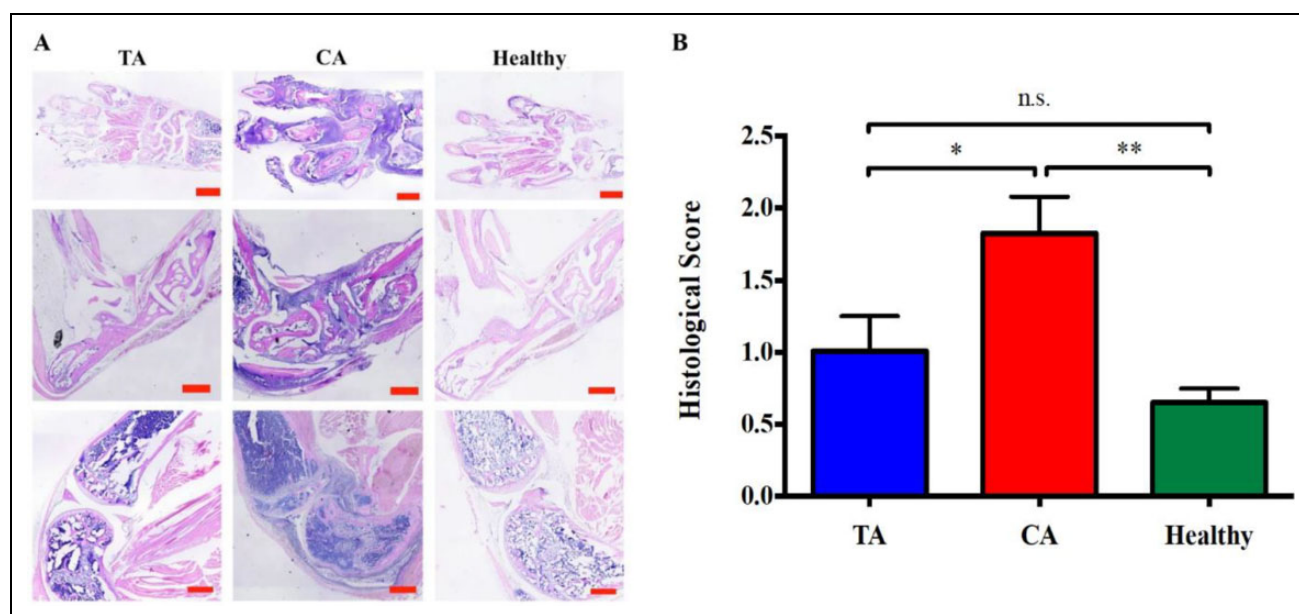
Figure 2. CA group mice had significantly better histological scores than those of TA group. (A) Representative pictures of histological sections. Scale bars = 500 μm. (B) Comparison of histological scores among three experimental groups at the end point (Day 42). Maximum score = 4. Mean ± standard error of the mean. TA group: $n = 10$, CA group: $n = 9$, Healthy group: $n = 4$. *$P < 0.05$, **$P < 0.01$ and n.s. = not significant.
CA: control assessment; TA: treatment assessment.

Table 2. Histological Scores (Day 42, Mean ± Standard Error of the Mean).

TA group ($n = 10$)	CA group ($n = 9$)	Healthy group ($n = 4$)
1.009 ± 0.243	1.826 ± 0.254	0.653 ± 0.097

CA: control assessment; TA: treatment assessment.

investigators every other day for 18 days. The averaged clinical score on Day 24 (the day of hUC-MSC infusion) for TA group was 7.08 (95% CI: 6.30, 7.86), 7.51 (95% CI: 6.73, 28.30) for CA group, and 0.38 (95% CI: −0.57, 1.33) for the Healthy group, respectively. The Day 24 Healthy group clinical scores were not significantly greater than zero ($P = 0.435$) and there was no significant difference in clinical scores between TA and CA groups, prior to treatment ($P = 0.126$) (Supplemental Table S1). The Day 24 clinical scores of both TA and CA groups were significantly higher than that of the Healthy group ($P < 0.0001$).

After infusion, a significant difference in clinical scores between TA and CA groups was detected on Day 28, i.e., 4 days after the hUC-MSC infusion (−1.53, $P = 0.003$, 95% CI: −2.29, −0.77; with Bonferroni correlation for multiple comparison, Supplemental Table S1) which continued to increase until Day 42 (end point) (−4.49, $P < 0.0001$, 95% CI: −5.97, −3.01; Table 3, Fig. 4 and Supplemental Fig. S2). In Batch 1, a significant difference in clinical scores between TA and CA groups was observable by Day 32 (−2.82,

$P = 0.036$, 95% CI: −4.52, −1.12) which continued to increase until Day 42 (end point) (−5.44, $P < 0.0001$, 95% CI: −7.40, −3.49) (Supplemental Table S2). In Batch 2, a significant difference in clinical scores between TA and CA groups started on Day 28 (−1.69, $P = 0.015$, 95% CI: −2.59, −0.79) and continued to increase until Day 38 (−3.95, $P = 0.012$, 95% CI: −6.02, −1.88) (Supplemental Table S3). All baseline clinical scores were zero.

When comparing the clinical scores between Day 24 and Day 42 (end point), a significant decrease of 3.12 ($P < 0.0001$, 95% CI: 2.04, 4.20) was observed in TA group, whereas the clinical score was significantly increased by an average of 1.13 ($P = 0.047$, 95% CI: 0.05, 2.21) 18 days after hUC-MSC infusion in CA group (Table 4). No significant change of clinical score was detected in Healthy group ($P = 0.668$, 95% CI: −2.18, 1.39; Table 5). Importantly, a significant difference in the 18-day clinical score trend was observed between TA and CA groups (−4.25, $P < 0.0001$, 95% CI: −5.78, −2.72; Table 5). Consistency was observed between both batches (Supplemental Tables S2 and S3).

A comparison between TA and CA group clinical scores over the time was also performed (Fig. 4 and Table 4). The model-based rate of change in clinical score was 1.86 decrease (95% CI: 1.58, 2.14) per 10 days in TA group and 0.60 increase (95% CI: 0.32, 0.88) per 10 days in CA group. Overall hUC-MSC infusion displayed a significant therapeutic effect on reducing clinical scores in a CIA murine model (−0.25 per day, $P < 0.0001$, 95% CI: −0.29, −0.21)
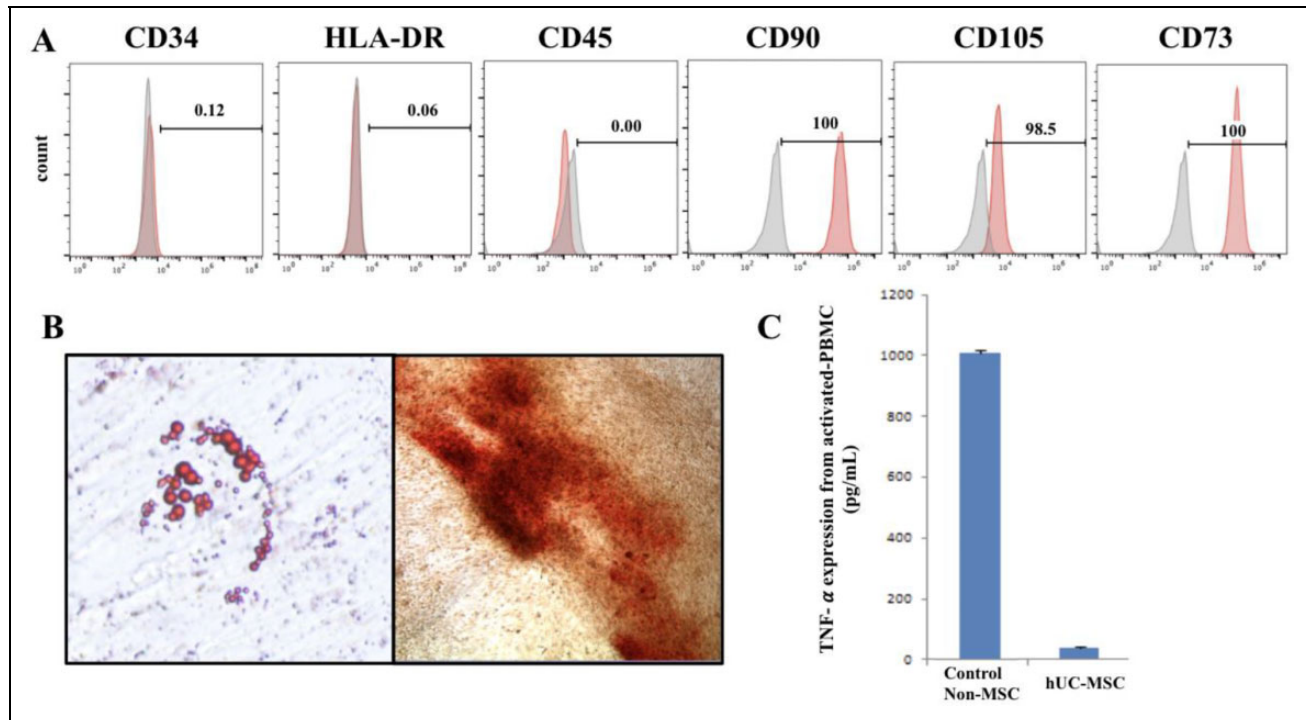
Figure 3. *In vitro* characterization of hUC-MSC. (A) Flow cytometric analysis showed that hUC-MSC were positive for the surface markers CD90, CD105, and CD73, while negative for CD34, HLA-DR, and CD45. (B) Oil Red staining (left) showed adipogenic potential of hUC-MSC after adipogenesis differentiation; Alizarin red staining (right) showed mineralization potential of hUC-MSC after osteogenic differentiation. (C) hUC-MSC showed a superior TNF-α-inhibitive effect when co-cultured with PBMC. TNF-α expression level was analyzed in the presence of hUC-MSC and a non-MSC control following activation of PBMC with anti-CD3, anti-CD28, and IL-2. Data are presented as mean ± standard deviation.
hUC-MSC: human umbilical cord tissue–derived mesenchymal stem cells; PBMC: peripheral blood mononuclear cells; TNF-α: tumor necrosis factor alpha.

Table 3. Clinical Scores After hUC-MSC Infusion (Combined Batches; Mean and 95% Confidence Interval).

| Time point	TA group	CA group	TA − CA	*P*-value
Day 26	7.17 (6.41, 7.94)	8.08 (7.31, 8.84)	−0.90 (−1.56, −0.24)	0.093
Day 28	6.81 (6.26, 7.37)	8.34 (7.79, 8.90)	−1.53 (−2.29, −0.77)	0.003
Day 30	6.55 (5.95, 7.15)	8.50 (7.90, 9.10)	−1.95 (−2.79, −1.10)	<0.001
Day 32	6.08 (5.04, 7.11)	8.78 (7.75, 9.81)	−2.70 (−3.74, −1.66)	<0.0001
Day 34	5.55 (4.55, 6.55)	8.53 (7.53, 9.53)	−2.97 (−4.07, −1.87)	<0.0001
Day 36	5.12 (3.50, 6.75)	8.85 (7.22, 10.48)	−3.73 (−4.98, −2.48)	<0.0001
Day 38	4.78 (3.35, 6.21)	9.02 (7.59, 10.46)	−4.25 (−5.63, −2.87)	<0.0001
Day 40	4.48 (3.25, 5.72)	8.79 (7.56, 10.03)	−4.31 (−5.68, −2.94)	<0.0001
Day 42	4.02 (2.95, 5.10)	8.52 (7.44, 9.59)	−4.49 (−5.97, −3.01)	<0.0001

CA: control assessment; hUC-MSC: human umbilical cord tissue–derived mesenchymal stem cells; TA: treatment assessment.

(Table 6). Similar results were also observed, showing consistency between batches. The trend detected in Healthy group was not significantly different compared to zero (−0.04 per day, $P > 0.05$, 95% CI: −0.09, 0.00). Representative pictures of paws are shown in Supplemental Fig. S3.

Joint swelling was measured with thickness gages (front and back paws) every other day for 18 days. On the day of hUC-MSC infusion (Day 24), paw thickness between TA and CA groups had no significant difference (−0.01 mm, $P = 0.874$, 95% CI: −0.16, 0.14). When analyzed separately, the thickness of neither front paws (0.03 mm, $P = 0.311$, 95% CI: −0.03, 0.08) nor hind paws (−0.05 mm, $P = 0.051$, 95% CI: −0.11, 0.00) showed significant difference between TA and CA groups.

The mean and 95% CI of paw thickness measured every 2 days after Day 24 were calculated for front and hind legs separately (Supplemental Table S4) and combined (Supplemental Table S5). No significant difference was observed in
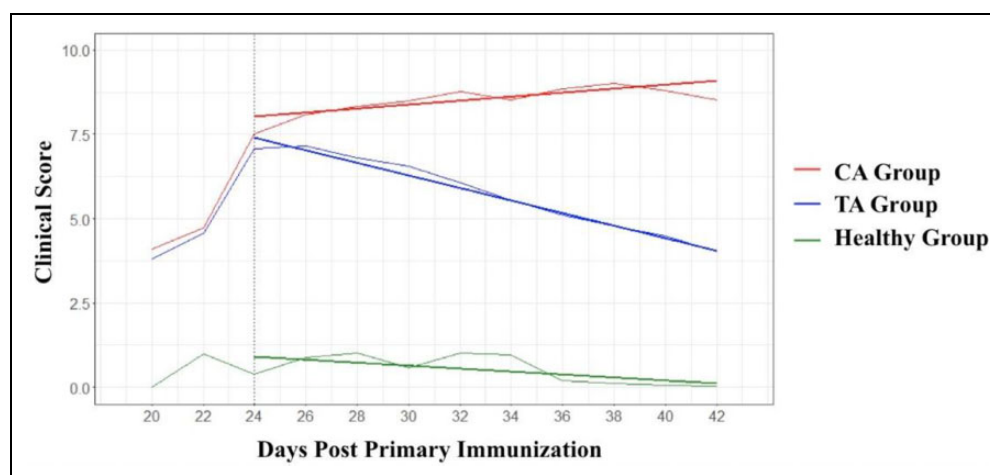
Figure 4. Average clinical score and model-based rate of change for each experimental group from Day 20 to Day 42 (two batches combined). TA group: $n = 21$, CA group: $n = 20$, Healthy group: $n = 7$. Human umbilical cord tissue–derived mesenchymal stem cells were infused on Day 24 (dash line). The three straight bold lines stand for the linear mixed model–fitted linear trends of clinical score in each group.
CA: control assessment; TA: treatment assessment.

overall, front, or hind paw thickness between TA and CA groups from Day 26 to Day 42 (Supplemental Fig. S4).

Microscopic Joint Inflammation Was Reduced After hUC-MSC Treatment

After end point, mice were sacrificed, and tissues were harvested so that histological analysis could be performed on the joints. Briefly, at the end point (Day 42), mice (Batch 1) were sacrificed and legs were harvested and processed, then assayed with H&E staining. The histological scores of TA group were significantly lower than those of CA group ($P < 0.05$) and had no significant difference compared to those of the Healthy group ($P > 0.05$), demonstrating a significant therapeutic effect of hUC-MSC on RA. A significant difference was also observed between CA group and Healthy group ($P < 0.01$; Table 2, Fig. 2). Collectively, arthritis symptoms were successfully established in mice, and hUC-MSC treatment showed improvements in several clinical parameters relating to arthritis.

IL-6 Level Was Declined by hUC-MSC Treatment

Blood was taken for cytokine analysis at multiple time points throughout the experiment. Briefly, murine blood (Batch 1) was harvested on the days before (Day 22) and after (Day 26) the hUC-MSC infusion, as well as on the baseline and the end point (Day 42). Concentrations of pro-inflammatory cytokines IFN-γ, IL-6, TNF-α, and IL-1β in plasma were measured with Luminex assay (Table 7). At the baseline, the cytokine levels were low and there was no significant difference between TA and CA groups. On Day 22, the concentrations of IFN-γ, IL-6, and TNF-α were highly

Table 4. Changes of Clinical Score Between Day 24 and Day 42 (Estimate = Day 42 − Day 24).

Group	Batch	Estimate	95% Confidence Interval	P-value
TA	Combined	−3.12	(−4.20, −2.04)	<0.0001
	Batch 1	−3.40	(−4.71, −2.09)	<0.0001
	Batch 2	−2.81	(−4.62, −1.00)	0.007
CA	Combined	1.13	(0.05, 2.21)	0.047
	Batch 1	1.72	(0.34, 3.10)	0.024
	Batch 2	0.60	(−1.12, 2.32)	0.502
Healthy	Combined	−0.39	(−2.18, 1.39)	0.668
	Batch 1	−0.69	(−2.76, 1.38)	0.522
	Batch 2	0.00	(−3.14, 3.14)	1.000

CA: control assessment; TA: treatment assessment.

increased with large variation among animals. The concentration of IL-1β also increased but not as high as the other cytokines. No significant difference was shown between TA and CA groups for all the cytokines (Supplemental Table S6).

Two days after hUC-MSC infusion (Day 26), the concentration of IL-6 in TA group had significantly declined by 80.0% ($P < 0.0001$) compared with Day 22, whereas no significant change was observed in CA group. The concentrations of TNF-α in TA group dropped significantly by 14.3% from Day 22 ($P < 0.05$) while a climbing trend was observed in CA group (increased by 13% compared to Day 22). The concentrations of IFN-γ and IL-1β also decreased compared with Day 22, but there was no significant difference between TA and CA groups.

At the end point (Day 42), the concentration of IL-6 was further reduced in both TA and CA groups. The decrease of IL-6 in TA group (by 93.4% compared to Day 22) was

Table 5. Comparison (TA vs. CA) of Clinical Score Between Day 24 and Day 42 (Estimate = TA − CA).

Batch	Estimate	95% Confidence interval	*P*-value
Combined	−4.25	(−5.78, −2.72)	<0.0001
Batch 1	−5.12	(−7.02, −3.22)	<0.0001
Batch 2	−3.41	(−5.90, −0.91)	0.015

CA: control assessment; TA: treatment assessment.

Table 6. Comparison (TA vs. CA) on Clinical Score Over the Time (Estimate = TA − CA).

Batch	Estimate (per day)	95% Confidence interval	*P*-value
Combined	−0.25	(−0.29, −0.21)	<0.0001
Batch 1	−0.30	(−0.35, −0.24)	<0.0001
Batch 2	−0.20	(−0.26, −0.14)	<0.0001

CA: control assessment; TA: treatment assessment.

significantly steeper than that of CA group (by 64.7% compared to Day 22) ($P < 0.05$; Table 7 and Fig. 5A). The concentration of TNF-α was also declined in both TA and CA groups at the end point but without significant difference between TA and CA groups (Table 7 and Fig. 5B). For the concentration of IFN-γ and IL-1β, no significant difference was detected between TA and CA groups ($P > 0.05$; Table 7, Fig. 5C, D).

No Side Effect Was Observed After hUC-MSC Administration

No abnormalities, including appearance, behavior, secretions, and excreta, were observed after infusion of hUC-MSC and no mice died from infusion of test agents. No erythema, edema, or exudation was observed at injection site, after infusion of test agent.

Animals were weighed every other day for 18 days. Variations in animal weights prior to CIA disease induction were insignificant (Supplemental Table S7). After CIA model induction, all animals lost weight, and began to recover after 2 days. No significant difference in body weight was observed at any time point between TA and CA groups ($P > 0.05$, Supplemental Table S8), but by end point, both groups had lower average body weight than healthy mice (Supplemental Fig. S1).

Discussion

Stem cell therapies have the capacity to treat disease more directly than standard small-molecule drugs, which tend to only treat symptoms. MSC are a type of adult stem cell with immunomodulatory capabilities and were the active component of the hUC-MSC injection we evaluated in this study. MSC have been investigated for their beneficial therapeutic effects in multiple diseases, including myocardial infarction, connective tissue, autoimmune, inflammatory, lung, and kidney diseases[27,28]. Additionally, MSC have been evaluated in many animal studies and human clinical trials of rheumatic diseases [22,29,30]. There has been great interest in using MSC to treat patients with RA for many years[31,32]. We recently performed a meta-analysis of MSC in the treatment of RA and found that there was much variability between studies, and the origin of MSC may significantly impact treatment outcome[22]. For example, human umbilical cord and adipose-derived MSC may be more effective against RA than MSC

from other sources. Overall, previous preclinical and clinical studies showed positive efficacy and tolerability and therefore warrant further investigation into the clinical benefits of MSC in RA[22,33]. This study aimed to evaluate the efficacy from a single infusion of hUC-MSC to treat RA in a CIA murine model via tail vein and thereby provide information for preclinical studies of BX-U001.

After a CIA model was established, the administration of hUC-MSC significantly reduced clinical scores of TA group ($P < 0.01$ starting from 6 days after hUC-MSC administration) compared to CA group. Clinical scores are a qualitative measure of joint appearance based on comparison to healthy animal joints. Generally, mice induced with a CIA model had swollen joints, and erythema around joints and extremities (especially in the hind legs). While paw thickness measurements alone showed no significant difference between TA and CA groups, these measurements are limited by the soft tissue surrounding the areas of inflammation and cannot tell us about the underlying joint structure. Clinical scoring includes color and overall appearance (straightness) of the joints, a general macroscopic evaluation that may indicate more about underlying joint health rather than the size of the joint alone.

In many studies of inflammation, histological evaluation can give insight to invasion of the immune system into specific tissue locations, and provide microscopic detail on structural damage, which macroscopic methods cannot achieve[34]. After treatment with hUC-MSC, the histological scores of the joints of TA group were significantly reduced compared to CA group ($P < 0.001$). The knee joint had significant inflammation and immune cell invasion in untreated CIA mice (CA group), and there tended to be reduced synovial fluid between the joints. Additionally, bone was clearly eroded in CA group joints, but had been at least partially protected in TA group joints. This type of damage is the typical manifestation of RA inflammation, and directly correlates with pain and overall joint function[35,36].

It is essential to evaluate the systemic effects of hUC-MSC treatment in RA, because the high levels of inflammatory cytokines released into the blood during RA pathogenesis can produce damage in the heart, lungs, and other vital organs, despite their geographical distance from inflamed joints[9,10]. In particular, TNF-α and IL-6 are key inflammatory cytokines in both the initial and advanced stages of RA disease[29,30]. The serum levels of these key cytokines were significantly reduced in hUC-MSC-treated

Table 7. Relative Concentrations of Cytokines (%, Mean $\pm$ Standard Error of the Mean).

Cytokines	Group	Time point		
		Before (Day 22)	After (Day 26)	End point (Day 42)
IFN-γ	TA	100.0 $\pm$ 0.0	37.5 $\pm$ 10.2	23.1 $\pm$ 8.3
	CA	100.0 $\pm$ 0.0	43.1 $\pm$ 11.3	25.2 $\pm$ 11.1
IL-6	TA	100.0 $\pm$ 0.0	20.0 $\pm$ 9.5[####]	6.6 $\pm$ 1.3*
	CA	100.0 $\pm$ 0.0	50.2 $\pm$ 20.0	35.3 $\pm$ 16.5
TNF-α	TA	100.0 $\pm$ 0.0	85.7 $\pm$ 6.7[#]	42.8 $\pm$ 6.9
	CA	100.0 $\pm$ 0.0	113.0 $\pm$ 16.5	50.1 $\pm$ 13.9
IL-1β	TA	100.0 $\pm$ 0.0	85.3 $\pm$ 8.4	74.9 $\pm$ 8.1
	CA	100.0 $\pm$ 0.0	77.5 $\pm$ 14.4	75.6 $\pm$ 13.3

[#]Significant reduction compared with Day 22; [###]Significant declined by 80.0% (P < 0.0001) compared with Day 22; *Significantly lower compared with CA group.
CA: control assessment; IFN-γ: interferon gamma; IL-1β: interleukin 1 beta; TA: treatment assessment; TNF-α: tumor necrosis factor alpha.
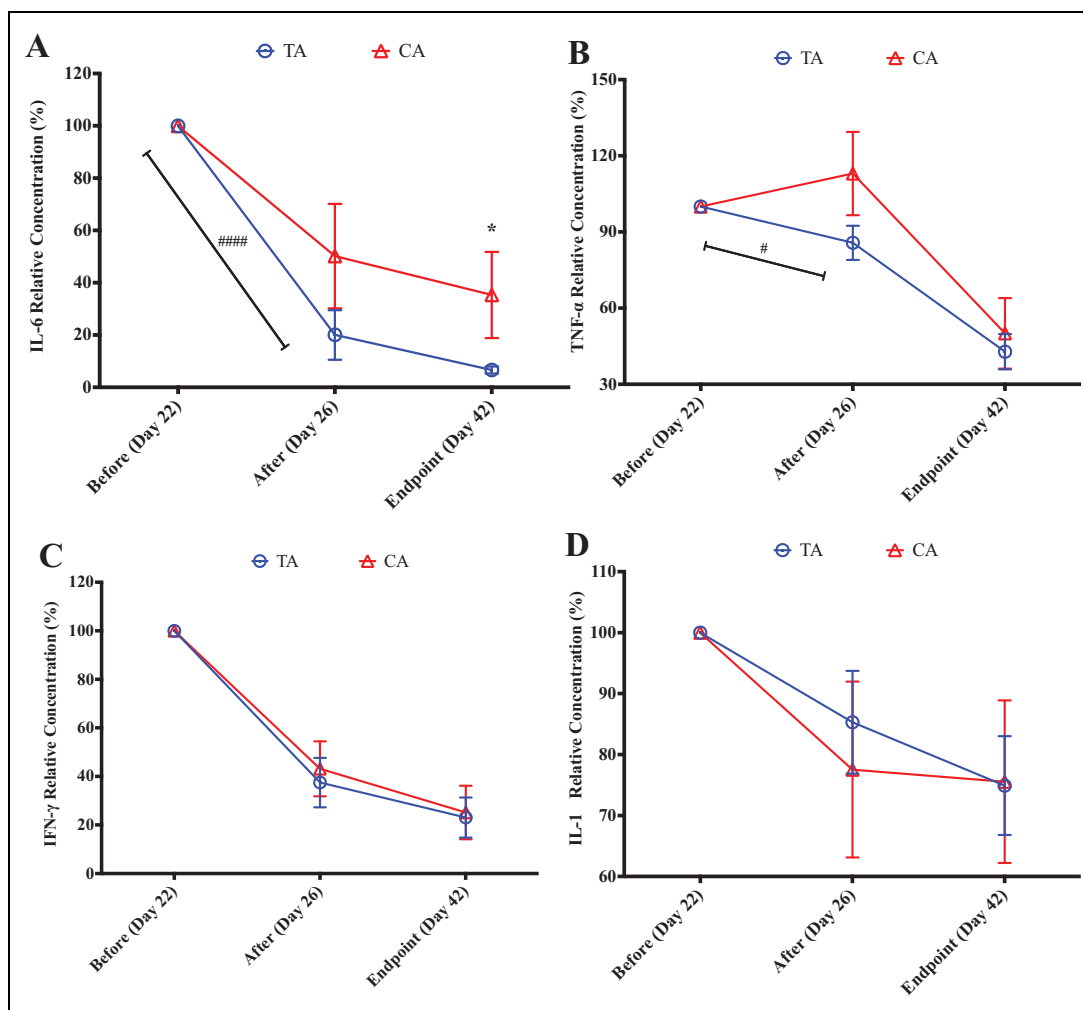
Figure 5. Concentrations of pro-inflammatory cytokines (IL-6, IFN-γ, TNF-α, and IL-1β) in each experimental group at baseline, Day 22, Day 26, and end point (Day 42). The concentrations of cytokines were determined by Luminex serology assay. Mean $\pm$ standard error of the mean. *P < 0.05 (TA group vs. CA group); [#]P < 0.05 and [####]P < 0.0001 (Day 22 vs. Day 26).
CA: control assessment; IFN-γ: interferon gamma; IL-6: interleukin 6; TA: treatment assessment; TNF-α: tumor necrosis factor alpha.

mice, compared to untreated controls. There was less of an effect of IFN-γ and IL-1β, which are also linked to RA pathophysiology. The link between MSC treatment and a reduction in TNF-α and IL-6 is likely attributable to their ability to influence systemic levels of M2 anti-inflammatory macrophages and upregulate the levels of FoxP3^{+} T-reg[29,37,38]. Immediately after intravenous injection, many MSC become trapped in the capillaries of the lungs, where they are engulfed by macrophages[39]. The effect MSC have on circulating macrophages, resulting from their engulfment, is heavily linked to the ratio of anti-inflammatory cytokines produced by these macrophages, and their downstream interactions with other immune cells[39–41]. The detailed mechanisms of hUC-MSC action on RA are still being elucidated, but the reduction of TNF-α and IL-6 cytokines appears to be a key feature.

While the hUC-MSC evaluated in this study did not treat every RA disease parameter tested, they did provide significant improvements in macroscopic (clinical scores) and microscopic (histology) pathophysiology, and reduced systemic levels of key inflammatory cytokines related to the RA. It is important to consider the application of cell therapies to disease as a supplement rather than a replacement to drug-based treatments. In many drug-resistant cases of autoimmune disease, MSC may provide a chance at treatment, where there is none. In RA patients who respond partially to drug treatments, MSC may provide an additional treatment option or alternative that might be less immunosuppressive or have as severe side effects as the current standard drug treatments methotrexate and TNF-α blockers.

Conclusion

A single intravenous infusion of BX-U001 hUC-MSC can significantly relieve RA disease symptoms in a CIA mouse model. hUC-MSC decreased clinical scores, histological scores, and serum levels of pro-inflammatory cytokines, indicating they have significant clinical potential. This new cell product showed no signs of adverse effects and will be further tested for safety and efficacy in clinical studies with human patients. The limitations of drug-based treatments may be overcome or at least supplemented by cell therapies, such as hUC-MSC.

Data Analysis and Statistics

Clinical scores were studied as the total scores of four legs whereas paw thickness was analyzed based on each leg separately due to the huge difference of the measurement between front and hind legs.

First, a linear mixed model (LMM) was used to examine the difference of outcome measures on infusion day (Day 24), among TA, CA, and Healthy groups, with adjustments for within-batch correlation. The LMM has the following form:

$$Y_{ij} = \beta_0 + \beta_1 X_{ij} + \mu_j Z_j + \epsilon_{ij}$$

where Y_{ij} is the outcome for mouse i in batch j, β_0 is a shared intercept term, β_1 represents the coefficient of experimental group, X_{ij} is the design matrix for the fixed-group effect. μ_j represents a random intercept term associated with each batch. Z_j is the design matrix for the random batch effect, and ϵ_{ij} is a normal distributed error term. Pairwise comparisons of Day 24 outcome measures among three experimental groups were then conducted using tests of contrast based on the LMM.

Second, a similar LMM followed by contrast testing was used to compare the 18-day change [from infusion day (Day 24) to the end point (Day 42)] of each outcome among the three groups. Unlike the previous model, the dependent variable Y_{ij} was altered to the 18-day outcome change. If a significant difference was observed in 18-day outcome change among the three groups, the different trends of changes over time were further examined by incorporating longitudinal data. The LMM used to compare the slopes has the following form:

$$Y_{ijk} = \beta_0 + \beta_1 X_{ij} + \beta_2 Day + \beta_3 X_{ij}*Day + \mu_j Z_j + \gamma_{i(j)} M_{i(j)} + \epsilon_{ijk}$$

where Y_{ijk} is the outcome for mouse i in batch j on Day k, β_0 is a shared intercept term, and β_1 to β_3 represent the coefficients of fixed effect. Similar to the previous model, μ_j represents a random intercept term associated with each batch. Z_j is the design matrix for the random batch effect. $\gamma_{i(j)}$ represents a random effect associated with each mouse, which is also nested in the batch effect. $M_{i(j)}$ is the design matrix for the random mouse effect, and ϵ_{ijk} is a normal distributed error term.

The slope of outcome change for each experimental group was calculated and the differences in slopes were compared using contrast testing. In order to investigate when a significant difference can be observed between TA and CA groups, the outcome measures on each measurement day were studied and compared. The difference between TA and CA groups was examined with a similar LMM model. Bonferroni correlation was applied to adjust for multiple-day comparisons.

For paw thickness, the abovementioned analysis first compared the overall mouse leg measurements among three groups without specifying the leg locations (front/hind). As paw thickness was quite different between front and hind legs, the measurements of front and hind legs were also studied separately. (1) Leg locations (front/hind) and (2) the interactions between leg locations and groups (TA/CA) were added into each of the above LMM, to allow for different treatment responses onto different leg locations.

The two batches were studied separately as a sensitivity analysis, to examine whether the results were robust and consistent in both batches. All the above analyses were repeated in each batch. A linear regression model was used instead of LMM for the comparisons on infusion day (Day 24), daily responses, and 18-day changes.

ORCID iD

Henry P. Farhoodi ![ORCID] https://orcid.org/0000-0003-1729-5418

Supplemental Material

Supplemental material for this article is available online.

References

1. Barbour KE. Vital signs: prevalence of doctor-diagnosed arthritis and arthritis-attributable activity limitation — United States, 2013–2015. MMWR Morb Mortal Wkly Rep. 2017; 66(9):246–253.
2. Hootman JM, Helmick CG, Barbour KE, Theis KA, Boring MA. Updated projected prevalence of self-reported doctor-diagnosed arthritis and arthritis-attributable activity limitation among US adults, 2015-2040. Arthritis Rheumatol. 2016; 68(7):1582–1587.
3. Gabriel SE, Crowson CS, O'Fallon WM. The epidemiology of rheumatoid arthritis in Rochester, Minnesota, 1955-1985. Arthritis Rheum. 1999;42(3):415–420.
4. Costenbader KH, Chang S-C, Laden F, Puett R, Karlson EW. Geographic variation in rheumatoid arthritis incidence among women in the United States. Arch Intern Med. 2008;168(15): 1664–1670.
5. Feldmann M, Brennan FM, Maini RN. Rheumatoid arthritis. Cell. 1996;85(3):307–310.
6. Scott DL, Wolfe F, Huizinga TW. Rheumatoid arthritis. Lancet. 2010;376(9746):1094–1108.
7. Ropes MW, Bennett GA, Cobb S, Jacox R, Jessar RA. 1958 Revision of diagnostic criteria for rheumatoid arthritis. Arthritis Rheum. 1959;2(1):16–20.
8. Arnett FC, Edworthy SM, Bloch DA, McShane DJ, Fries JF, Cooper NS, Healey LA, Kaplan SR, Liang MH, Luthra HS. The American Rheumatism Association 1987 revised criteria for the classification of rheumatoid arthritis. Arthritis Rheum. 1988;31(3):315–324.
9. Smolen JS, Aletaha D, Redlich K. The pathogenesis of rheumatoid arthritis: new insights from old clinical data? Nat Rev Rheumatol. 2012;8(4):235–243.
10. Choy E. Understanding the dynamics: pathways involved in the pathogenesis of rheumatoid arthritis. Rheumatology (Oxford). 2012;51(suppl_5):v3–v11.
11. van der Linden MPM, van der Woude D, Ioan-Facsinay A, Levarht EWN, Stoeken-Rijsbergen G, Huizinga TWJ, Toes REM, van der Helm-van Mil AHM. Value of anti-modified citrullinated vimentin and third-generation anti-cyclic citrullinated peptide compared with second-generation anti-cyclic citrullinated peptide and rheumatoid factor in predicting disease outcome in undifferentiated arthritis and rheumatoid arthritis. Arthritis Rheum. 2009;60(8):2232–2241.
12. Kinne RW, Bräuer R, Stuhlmüller B, Palombo-Kinne E, Burmester G-R. Macrophages in rheumatoid arthritis. Arthritis Res. 2000;2(3):189–202.
13. Sun W, Zhang H, Wang H, Chiu YG, Wang M, Ritchlin CT, Kiernan A, Boyce BF, Xing L. Targeting notch-activated M1 macrophages attenuates joint tissue damage in a mouse model of inflammatory arthritis. J Bone Miner Res. 2017;32(7): 1469–1480.
14. Culemann S, Grüneboom A, Nicolás-Ávila JÁ, Weidner D, Lammle KF, Rothe T, Quintana JA, Kirchner P, Krljanac B, Eberhardt M, Ferrazzi F, et al. Locally renewing resident synovial macrophages provide a protective barrier for the joint. Nature. 2019;572(7771):670–675.
15. Paoletti A, Rohmer J, Ly B, Pascaud J, Riviere E, Seror R, Le Goff B, Nocturne G, Mariette X. Monocyte/Macrophage abnormalities specific to rheumatoid arthritis are linked to miR-155 and are differentially modulated by different TNF inhibitors. J Immunol. 2019;203(7):1766–1775.
16. van Oosterhout M, Bajema I, Levarht EWN, Toes REM, Huizinga TWJ, van Laar JM. Differences in synovial tissue infiltrates between anti–cyclic citrullinated peptide–positive rheumatoid arthritis and anti–cyclic citrullinated peptide–negative rheumatoid arthritis. Arthritis Rheum. 2008;58(1):53–60.
17. Vossenaar ER, Smeets TJM, Kraan MC, Raats JM, Venrooij WJV, Tak PP. The presence of citrullinated proteins is not specific for rheumatoid synovial tissue. Arthritis Rheum. 2004;50(11):3485–3494.
18. van der Helm-van Mil AH, Verpoort KN, Breedveld FC, Toes RE, Huizinga TW. Antibodies to citrullinated proteins and differences in clinical progression of rheumatoid arthritis. Arthritis Res Ther. 2005;7(5):R949–R958.
19. Bjarnason I, Hayllar J, MacPherson AJ, Russell AS. Side effects of nonsteroidal anti-inflammatory drugs on the small

and large intestine in humans. Gastroenterology. 1993;104(6): 1832–1847.

20. Le Blanc K, Frassoni F, Ball L, Locatelli F, Roelofs H, Lewis I, Lanini E, Sundberg B, Bernardo ME, Remberger M, Dini G, et al. Mesenchymal stem cells for treatment of steroid-resistant, severe, acute graft-versus-host disease: a phase II study. Lancet. 2008;371(9624):1579–1586.

21. Fan C-G, Zhang Q, Zhou J. Therapeutic potentials of mesenchymal stem cells derived from human umbilical cord. Stem Cell Rev Rep. 2011;7(1):195–207.

22. Liu L, Wong CW, Han M, Farhoodi HP, Liu G, Liu Y, Liao W, Zhao W. Meta-analysis of preclinical studies of mesenchymal stromal cells to treat rheumatoid arthritis. EBioMedicine. 2019;47:563–577.

23. Chandrashekara S.The treatment strategies of autoimmune disease may need a different approach from conventional protocol: a review. Indian J Pharmacol. 2012;44(6):665–671.

24. Ghannam S, Bouffi C, Djouad F, Jorgensen C, Noël D. Immunosuppression by mesenchymal stem cells: mechanisms and clinical applications. Stem Cell Res Ther. 2010;1(1):2.

25. Lu LL, Liu YJ, Yang SG, Zhao QJ, Wang X, Gong W, Han ZB, Xu ZS, Lu YX, Liu D, Chen ZZ, et al. Isolation and characterization of human umbilical cord mesenchymal stem cells with hematopoiesis-supportive function and other potentials. Haematologica. 2006;91(8):1017–1026.

26. Pietrosimone KM, Jin M, Poston B, Liu P. Collagen-induced arthritis: a model for murine autoimmune arthritis. Bio Protoc. 2015;5(20):e1626.

27. Liu H, Ding J, Wang J, Wang Y, Yang M, Zhang Y, Chang F, Chen X. Remission of collagen-induced arthritis through combination therapy of microfracture and transplantation of thermogel-encapsulated bone marrow mesenchymal stem cells. PLos One. 2015;10(3):e0120596.

28. Tyndall A. Mesenchymal stem cell treatments in rheumatology—a glass half full? Nat Rev Rheumatol. 2014;10(2): 117–124.

29. Wang L, Wang L, Cong X, Liu G, Zhou J, Bai B, Li Y, Bai W, Li M, Ji H, Zhu D, et al. Human umbilical cord mesenchymal stem cell therapy for patients with active rheumatoid arthritis: safety and efficacy. Stem Cells Dev. 2013;22(24):3192–3202.

30. Wang L, Zhang Y, Li H, Hong J, Chen X, Li M, Bai W, Wang J, Liu Y, Wu M. Clinical observation of employment of umbilical cord derived mesenchymal stem cell for juvenile idiopathic arthritis therapy. Stem Cells Int. 2016;2016:9165267.

31. Liang J, Li X, Zhang H, Wang D, Feng X, Wang H, Hua B, Liu B, Sun L. Allogeneic mesenchymal stem cells transplantation in patients with refractory RA. Clin Rheumatol. 2012;31(1): 157–161.

32. Álvaro-Gracia JM, Jover JA, García-Vicuña R, Carreño L, Alonso A, Marsal S, Blanco F, Martinez-Taboada VM, Taylor P, Martin-Martin C, DelaRosa O, et al. Intravenous administration of expanded allogeneic adipose-derived mesenchymal stem cells in refractory rheumatoid arthritis (Cx611): results of a multicentre, dose escalation, randomised, single-blind, placebo-controlled phase Ib/IIa clinical trial. Ann Rheum Dis. 2017;76(1):196–202.

33. Zhou B, Yuan J, Zhou Y, Ghawji M, Deng YP, Lee AJ, Lee AJ, Nair U, Kang AH, Brand DD, Yoo TJ. Administering human adipose-derived mesenchymal stem cells to prevent and treat experimental arthritis. Clin Immunol. 2011;141(3):328–337.

34. Garimella MG, Kour S, Piprode V, Mittal M, Kumar A, Rani L, Pote ST, Mishra GC, Chattopadhyay N, Wani MR. Adipose-derived mesenchymal stem cells prevent systemic bone loss in collagen-induced arthritis. J Immunol. 2015;195(11): 5136–5148.

35. Welsing PMJ, Gestel AMV, Swinkels HL, Kiemeney LALM, Riel PLCMV. The relationship between disease activity, joint destruction, and functional capacity over the course of rheumatoid arthritis. Arthritis Rheum. 2001;44(9):2009–2017.

36. Ødegård S, Landewé R, van der Heijde D, Kvien TK, Mowinckel P, Uhlig T. Association of early radiographic damage with impaired physical function in rheumatoid arthritis: a ten-year, longitudinal observational study in 238 patients. Arthritis Rheum. 2006;54(1):68–75.

37. Vasandan AB, Jahnavi S, Shashank C, Prasad P, Kumar A, Prasanna SJ. Human mesenchymal stem cells program macrophage plasticity by altering their metabolic status via a PGE 2 -dependent mechanism. Sci Rep. 2016;6(1):38308.

38. Weiss ARR, Dahlke MH. Immunomodulation by Mesenchymal Stem Cells (MSCs): mechanisms of action of living, apoptotic, and dead MSCs. Front Immunol. 2019;10:1191.

39. De Witte SFH, Luk F, Parraga JMS, Gargesha M, Merino A, Korevaar SS, Shankar AS, O'Flynn L, Elliman SJ, Roy D, Betjes MGH, et al. Immunomodulation by therapeutic Mesenchymal Stromal Cells (MSC) is triggered through phagocytosis of MSC by monocytic cells. Stem Cells. 2018;36(4): 602–615.

40. Luk F, De Witte SFH, Korevaar SS, Roemeling-van Rhijn M, Franquesa M, Strini T, van den Engel S, Gargesha M, Roy D, Dor FJMF, Horwitz EM, et al. Inactivated mesenchymal stem cells maintain immunomodulatory capacity. Stem Cells Dev. 2016;25(18):1342–1354.

41. Gonçalves F da C, Luk F, Korevaar SS, Bouzid R, Paz AH, Lopez-Iglesias C, Baan CC, Merino A, Hoogduijn MJ. Membrane particles generated from mesenchymal stromal cells modulate immune responses by selective targeting of pro-inflammatory monocytes. Sci Rep. 2017;7(1):12100.